Stacking the Equiangular Spiral

Arti Agrawal, Y. O. Azabi and B. M. A. Rahman

***Abstract*— We present an algorithm that adapts the mature Stack and Draw (SaD) methodology for fabricating the exotic Equiangular Spiral Photonic Crystal Fiber. (ES-PCF) The principle of Steiner chains and circle packing is exploited to obtain a non-hexagonal design using a stacking procedure based on Hexagonal Close Packing. The optical properties of the proposed structure are promising for SuperContinuum Generation. This approach could make accessible not only the equiangular spiral but also other quasi-crystal PCF through SaD.**

***Index Terms*—Equiangular Spiral, Photonic Crystal Fiber, Stack and Draw.**

I. Introduction

QUASI Crystal Photonic Crystal Fiber (QC-PCF) designs have been proposed for many different applications and to obtain desired modal properties [1]-[5]. Such properties could include flat dispersion [1], high non-linearity [2], large birefringence [3], increased optical through put [4], mode discrimination for fiber lasers [5] and others that may not be realizable with conventional periodic structures. Thus there is some merit in exploring non-hexagonal templates amongst PCF. A common challenge with many of these designs is that of fabrication.

Methods like Stack and Draw (SaD) [6] that are well understood and used widely may be difficult to apply for non-hexagonal designs. While techniques such as drilling [7] and extrusion [8] offer alternative approaches, the concerns with utilizing these are the design complexity that can be handled, potential cost and thus availability to a large number of users.

Recently some optical properties of the unconventional Equiangular Spiral PCF (ES-PCF) design were presented and it was shown that this design offers excellent control over the modal properties [9, 10]. It would be possible to obtain small modal area (leading to enhanced non-linearity) with simultaneously small, flat dispersion in the ES-PCF, making it suitable for non-linear applications such as SuperContinuum Generation (SCG) [11]. Further, it was shown that the bending loss in ES-PCF could be much lower than conventional Hexagonal PCF (H-PCF) for small d/pitch values [10]. However, like some other non-hexagonal, QC fiber designs, the ES-PCF has not yet been fabricated.

In this article, we present an algorithm for the fabrication of the ES-PCF structure by adapting the well established SaD technology. Furthermore, we present simulation results for the ES-PCF structure obtained by means of the proposed algorithm.

Manuscript received March 13, 2012.

The authors are with the School of Engineering and Mathematical Sciences, City University London, Northampton Square, London, EC1V 0HB, UK (phone: +44(0)2070408366; e-mail: arti.agrawal.1@ city.ac.uk).

II. Fabrication Algorithm

The SaD method consists of stacking capillaries/rods in a repeating hexagonal arrangement to obtain a perform that is drawn to fiber with application of heat and pressure. The underlying mathematical basis of SaD is the Hexagonal Close Packing (HCP) of circles in a plane (considering the transverse cross section of the PCF), which also results in the densest lattice packing in two dimensions [12]. A key requirement of the SaD procedure is that all the capillaries/rods need support, obtained through resting against other capillaries/rods. Furthermore, tubes/rods can only be placed in the depressions formed between existing tubes/rods, forcing the angle between these features to a fixed value of 60^o. Thus, irregular and non-hexagonal arrangements may seem very difficult to achieve with SaD. We show, however, how quasi-crystal designs such as the ES-PCF can be obtained through SaD.

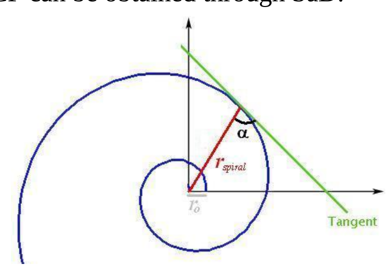

Fig. 1. The schematic of an equiangular spiral curve.

Fig. 1 shows a schematic of an Equiangular Spiral (ES) curve. This curve is governed by Eq. 1

$$r_{spiral} = r_o e^{\theta \cot\alpha} \quad (1)$$

where r_{spiral} is the distance of any point on the curve from the origin, r_o is the spiral radius, α is the angle between the tangent and the radial line and θ is the angle with the x-axis. The radii drawn at equal intervals of θ are in a geometric progression.

In the ES-PCF, the air holes are arranged in arms, where each arm is an ES. The air holes in each arm are located at positions determined by Eq. 1 for fixed values of r_o and θ. In every arm each air hole is separated by an angular increment θ with respect to the previous/successive air hole in the same arm.

An elegant way to adapt the SaD method for the ES-PCF is by use of the concept of Steiner chains [13]- given two concentric circles it is possible to fit into the annular region between them circles of equal radii that just touch each other.

By building an appropriate Steiner chain of capillaries around the core, the objective is to ensure that the capillaries are located at the coordinates determined by Eq. 1, and form an accurate representation of equiangular spirals. Each capillary ought to subtend an angle 2θ at the centre of the structure. Also, the angular increment between successive capillaries (air holes) in the same arm should be θ. This angle, θ, is determined by the number of arms, n.

$$\theta = 360^o / 2n \qquad (2)$$

Therefore, the capillaries (air holes) no longer fall on locations determined by a hexagonal template but according to the ES design. The stacking procedure to achieve the design is described below in detail.

The first step is placing a rod (core) surrounded by a tube (casing) which encloses the 1st and 2nd rings of air holes of all arms [see Fig. 2(a)]. In the annular region the capillaries have to be stacked to form the 1st two rings of the cladding. The distance between the centers of the 1s t and 2nd air holes in the same arm is calculated, the result of dividing it by 2 gives the outer radius of the tubes (air hole), r_hole_{out}. The radius of the rod (core) can then be defined as:

$$r_{core} = r_o - r\_hole_{out} \qquad (3)$$

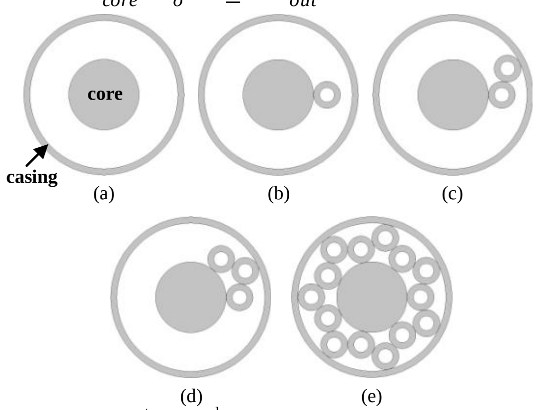

Fig. 2. Placement of 1st and 2nd ring capillaries in the ES-PCF by stacking; (a) rod (core) and tube (casing), (b) placing 1st air hole of 1st arm, (c) placing 2nd air hole of 1st arm, (d) placing 1st air hole of 2nd arm, (e) 1st and 2nd air holes of all arms are stacked.

The second step is placing a tube (air hole) such that it touches the central rod [see Fig. 2(b)] and a 2nd tube (air hole) such that it touches the casing and the 1st tube (air hole) [see Fig 2(c)]. This procedure is to be followed for all arms to stack tubes that form the first two rings as shown in Figures 2(d)-(e).

The capillaries that touch the central rod (core) form the first ring of the air-holes while the capillaries that touch the casing (and not the core) form the second ring of air holes. In the resulting structure no capillary is left free standing. Furthermore, this stacking ensures each tube (air hole) is placed as per Eq. 1 and the angular increment between air holes 1 and 2 of the same arm is exactly θ. The size and location of the air holes in the first two rings is important in the modal properties such as dispersion. However, the location of the air holes in the third ring (in terms of angle with respect to the origin) does not have much effect on dispersion and effective area (A_{eff}) for the ES-PCF. Therefore, their placement can be relatively flexible. Furthermore, to lower the leakage loss we show how to stack large capillaries in the outer 3rd ring [14].

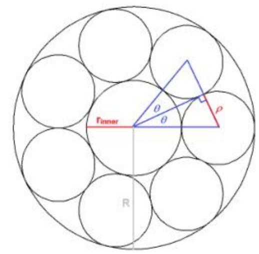

Fig. 3. Steiner chain of circles filling the gap between 2 concentric circles.

The stacking of the 3rd ring air holes repeats the use of Steiner chain concept shown in Fig. 3 (where R is radius of the outer circle, r_{inner} is the radius of the inner circle, and ρ is the radius of the enclosed circles in the annular region) which indicates that:

$$\frac{R}{r_{inner}} = \frac{1+\sin(\theta)}{1-\sin(\theta)} = x \qquad (4)$$

using

$$\sin(\theta) = \rho / (r_{inner} + \rho) \qquad (5)$$

and substituting Eq.5. in Eq.4 results in the formula which defines the outer radius of the 3rd ring capillaries as:

$$\rho = r_{inner} \times ((x-1)/2) \qquad (6)$$

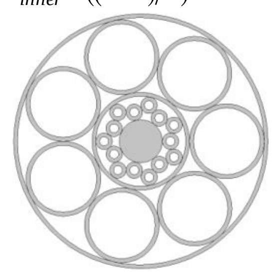

Fig. 4. The cross section of all stacked tubes and rods for exotic equiangular spiral PCF structure of 7 arms.

Fig. 4 shows the ES-PCF structure that would be obtained by implementing this algorithm. It should be noted that the algorithm can be generalized for any number of arms and the core and air hole sizes can be varied to suit the needs of the optical design.

There is a degree of challenge associated with the complexity in stacking and producing rods/capillaries of required dimensions in realizing the ES-PCF design, however, with some effort it can be met, for example by using sand technology where vertical stacking is possible [15]. Although the fabrication algorithm addresses the ES design specifically, the concept indicates that quasi-crystal designs can be produced through stacking.

III. Results

In this section we show some simulation results for optical properties of the ES-PCF structure obtained by the proposed algorithm using the full vectorial FEM method [16]. About 15000 second order elements arranged in an irregular mesh have been used to represent the structure. The properties of the modal field of the ES-PCF such as A_{eff}, non-linearity (γ) variation with core diameter and dispersion behaviour as a function of wavelength are presented. We use the definition given in [17] to calculate A_{eff}. Dispersion and nonlinearity are calculated as per the formulae in [1] and [18], respectively.

The simulations are for PCF in SF57 glass and in this instance pertain to a structure optimized for SCG pumped at 1064*nm*. The fiber parameters are: $r_o=0.5\mu m$, radius of air holes in the 1st and 2nd rings is $0.1375\mu m$, radius of 3rd ring air holes is $0.5528\mu m$, $\theta=25.7^o$, number of arms=*7*.

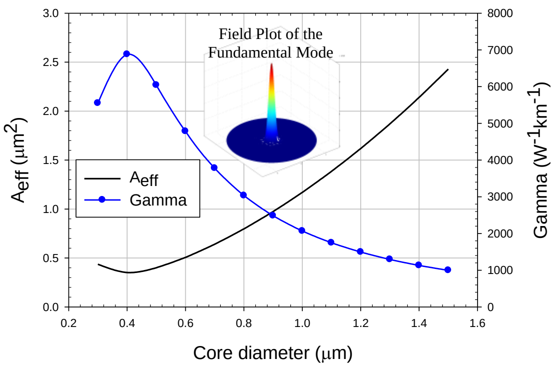

Fig. 5. Variation of γ and A_{eff} with core diameter for the ES-PCF.

Fig. 5 shows the variation in the A_{eff} as a function of the core diameter as well as the corresponding γ values, where the air filling fraction is kept constant ($r/r_o=0.275$). The smallest possible value of the effective area at the operating wavelength of *1064nm* is $\sim 0.352\mu m^2$. The associated γ value is $6878\ W^{-1}km^{-1}$, which is one of the largest yet proposed in SF57 PCF in comparison with $A_{eff}=0.84\mu m^2$ and $\gamma\sim 3000\ W^{-1}km^{-1}$, with the same core diameter published in [18]. The dispersion associated with the fiber ($r_o=0.5\mu m$) is shown in Fig. 6. The absolute value of dispersion at the pump wavelength of interest is D~*6.7ps/km/nm* with slope ~*1.16ps/km/nm*^{2}, compared to D>~ *50ps/km/nm* with a steep slope (Fig.3, Ref. 18). Hence, the ES-PCF offers both a high degree of modal confinement (large γ) and small, flat dispersion near the pump wavelength even though the index contrast between the glass material and air is quite large. These properties make the proposed structure extremely suitable for SCG.

IV. Conclusion

We have presented an algorithm for fabrication of a non traditional PCF design, the ES-PCF which offers excellent performance over several characteristics, especially effective modal area and dispersion, both key for broadband SCG. The ES-PCF can be useful for SCG for the mid and far IR wavelength regimes that are important in astrophotonics, sensing and spectroscopy. New materials such as chalcogenides could be used more effectively with good control of the modal field, even when the index contrast is significant. Both solid core and hollow core ES-PCF can be realized with the algorithm presented. Whereas previously, stacking did not seem to be a feasible procedure, we have shown that it can be adapted even for non-hexagonal designs. Hence it can open the door to realising quasi crystal designs.

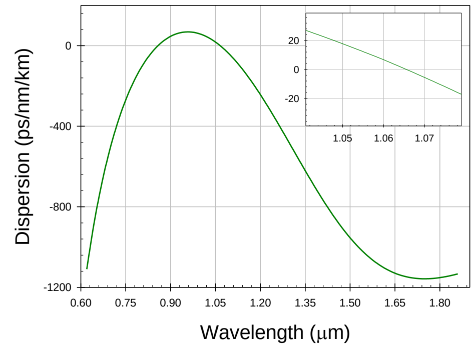

Fig. 6. Dispersion variation with wavelength for Equiangular Spiral PCF.

References

[1] S. Kim, and C-S. Kee, "Dispersion properties of dual-core photonic-quasicrystal fiber," *Opt. Express* vol. 17, pp.15885-15890, 2009.

[2] J. Park, J. Kim, S. Lee, S. Kim, and K. Oh, "Ultra-flattened Dispersion and high nonlinearity in a square lattice photonic crystal fiber," in *15th OptoElectronics and Communications Conference*, Japan, paper 7P-42.

[3] L. An, Z. Zheng, Z. Li, T. Zhou, and J. Cheng, "Ultrahigh birefringent photonic crystal fiber with ultralow confinement loss using four airholes in the core," *J. Lightw. Technol.* vol. 27, pp. 3175-3180, 2009.

[4] S. T. Huntington, B. C. Gibson, J. Canning, K. Digweed-Lyytikainen, J. D. Love, and V. Steblina, "A fractal-based fiber for ultra-high throughput optical probes," *Opt. Express* vol. 15, pp. 2468-2475, 2007.

[5] F. Stutzki, F. Jansen, C. Jauregui, J. Limpert, and A. Tunnermann, "Non-hexagonal large-pitch fibers for enhanced mode discrimination," *Opt. Express* vol. 19, pp. 12081-12086, 2011.

[6] J. C. Knight, T. A. Birks, P. St. J. Russell, and D. M. Atkin, "All-silica single-mode optical fiber with photonic crystal cladding," *Opt. Lett.* vol. 21, pp. 1547-1549, 1996.

[7] X. Feng, A. K. Mairaj, D. Hewak, and T. M. Monro, "Nonsilica glasses for holey fibers," *J. Lightw. Technol.* vol. 23, pp. 2046-2054, 2005.

[8] H. Ebendorff-Heiderpriem, Y. Li, and T. M. Monro, "Reduced loss in extruded soft glass microstructured fiber," *Electro. Lett.* vol. 43, pp.1343-1345, 2007.

[9] A. Agrawal, N. Kejalakshmy, B. M. A. Rahman, and K. T. V. Grattan, "Soft glass equiangular spiral photonic crystal fiber for supercontinuum generation," *IEEE Photon. Technol. Lett.* vol. 21, pp. 1722-1724, 2009.

[10] A. Agrawal, N. Kejalakshmy, M. Uthman, B. M. A. Rahman, A. Kumar, and K. T. V. Grattan, "Ultra low bending loss equiangular spiral photonic crystal fibers in the terahertz regime," *AIP Advances* vol. 2, pp. 022140, 2012.

[11] J. M. Dudley, G. Genty, and S. Coen, "Supercontinuum generation in photonic crystal fiber," *Rev. of Mod. Phys.* vol. 78, pp. 1135-1184, 2006.

[12] J. H. Conway, and N. J. A. Sloane, *Sphere Packings, Lattices, and Groups*, 2nd ed. (Springer-Verlag, 1993).

[13] C. S. Ogilvy, *Excursions In Geometry Ch. 4* (Dover, New York, 1990).

[14] F. Poli, A. Cucinotta, and S. Selleri, *Photonic Crystal Fibers Properties and Applications Ch. 1* (Springer, The Netherlands, 2007).

[15] A. Giraud, F. Sandoz, and J. Pelkonen, "Innovation in preform fabrication technologies," in *14th OptoElectronics and Communications Conference (OECC2009)*, Hong Kong, paper ThM1.

[16] N. Kejalakshmy, B. M. A. Rahman, A. Agrawal, T. Wongcharoen, and K. T. V. Grattan, "Characterization of single-polarization single-mode photonic crystal fiber using full-vectorial finite element method," *Appl. Phys. B* vol. 93, pp.223-230, 2008.

[17] B. M. A. Rahman, N. Kejalakshmy, M. Utman, A. Agrawal, T. Wongcharoen, and K. T. V. Grattan, "Mode degeneration in bent photonic crystal fiber study by using the finite element method," *Appl. Opt.* vol. 48, pp. G131-G138, 2009.

[18] J. Y. Y. Leong, P. Petropoulous, J. H. Price, H. Ebendorff-Heiderpriem, S. Asimakis, R. C. Moore, K. Frampton, V. Finazzi, X. Feng, T. M. Monro, and D. J. Richardson, "High-nonlinearity dispersion-shifted lead-silicate holey fibers for efficient 1-µm pumped supercontinuum generation," *J. Lightw. Technol.*, vol. 24, pp. 183–190, 2006.